Primljen / Received: 12.10.2022.
Ispravljen / Corrected: 2.4.2023.
Prihvaćen / Accepted: 11.4.2023.
Dostupno online / Available online: 10.7.2023.

Damage assessment, fragility, and vulnerability analysis of reinforced concrete building

Authors:

Prof.emer. Radomir Folić, PhD. CE
University of Novi Sad, Serbia
Faculty of Technical Sciences
boris.r.folic@gmal.com
Corresponding author

Miloš Čokić, PhD. CE
Termoenergo Inženjering, Serbia
cokicmilos@gmail.com

Boris Folić, PhD. CE
University of Belgrade, Serbia
Innovation Centre
Faculty of Mechanical Engineering
boris.folic@gmail.com

Assoc.Prof. Zoran Brujić, dipl.ing.građ.
University of Novi Sad, Serbia
Faculty of Technical Sciences
zbrujic@uns.ac.rs

Subject review

Radomir Folić, Miloš Čokić, Boris Folić, Zoran Brujić

Damage assessment, fragility, and vulnerability analysis of reinforced concrete building

In addition to a concise literature review, this study presents a comparative analysis of reinforced concrete (RC) buildings through damage index (DI) analysis using different methodologies. The seismic response of a five-story RC frame system building, designed in accordance with the EN structural Eurocodes, was analysed through fragility and vulnerability assessments. The Park–Ang methodology was used in the analysis for determining DI and its parameters. Nonlinear static analysis (NSA) and nonlinear dynamic analyses (NDA) were performed, and the fragility and vulnerability curves were constructed using the obtained results and processed through statistical analysis. The results were calculated using four different DI models: the DIPA model using both the NSA and NDA results (M1), modified DIPA model using both the NSA and NDA results (M2), DIPA model using the NSA results (M3), and modified DIPA model using the NSA results (M4).

Key words:
RC framed building, seismic nonlinear analyses, damage index assessment, fragility, vulnerability

Pregledni rad

Radomir Folić, Miloš Čokić, Boris Folić, Zoran Brujić

Procjena oštećenja i analiza vjerojatnosti oštećenja i oštetljivosti armiranobetonske zgrade

Osim sažetoga pregleda literature, rad sadrži komparativnu analizu armiranobetonskih (AB) zgrada pomoću analize indeksa oštećenja (DI) primjenom različitih metodologija. Seizmički odziv peterokatne okvirne AB zgrade, projektirane u skladu s konstrukcijskim normama Eurokod, analiziran je procjenom vjerojatnosti oštećenja i oštetljivosti. U analizi kojoj je cilj određivanje DI-ja i njegovih parametara primijenjena je metodologija Park–Ang. Provedene su nelinearna statička analiza (NSA) i nelinearna dinamička analiza (NDA) te su na temelju dobivenih rezultata oblikovane krivulje vjerojatnosti oštećenja i oštetljivosti koje su obrađene statističkom analizom. Rezultati su izračunani pomoću četiri različita modela DI-ja: model DIPA primjenom rezultata NSA i NDA (M1), modificirani model DIPA primjenom rezultata NSA i NDA (M2), model DIPA primjenom rezultata NSA (M3), te modificirani model DIPA primjenom rezultata NSA (M4).

Ključne riječi:
okvirna AB zgrada, seizmička nelinearna analiza, procjena indeksa oštećenja, vjerojatnost oštećenja, oštetljivost

1. Introduction

During strong earthquakes, the response of reinforced concrete (RC) structures can cause various types of damage. Therefore, the modern concept of designing seismically resistant structures requires nonlinear analysis, and performance-based design methods have been developed to address the damage and failure. Various levels of loss may occur depending on the degree of structural damage. Therefore, it is crucial to mitigate earthquake-induced damage to structures and minimise the loss of life and property.

The references cited in this paper pertain to the damage in RC structures, including moment-resistant frames (MRF). Several studies have referred to the development of performance-based design and assessment of seismic performance in RC structures, and their fragility and vulnerability issues have been more widely analysed.

An overview of seismic reliability and risk assessment based on fragility analysis was presented in [1], whereas guidelines for the fragility, vulnerability, and risk analysis of structures were presented in [2]. Analytical vulnerability assessment guidelines for low- to mid-rise buildings are outlined in [3]. A broader analysis of seismic fragility evaluation is the subject of [4], and analytical fragility methods for seismic risk assessment are presented in [5]. The use of the pushover method for the seismic design of structures and an assessment of existing structures was described in [6].

In [7], seismic damage indices for RC buildings and related concepts and procedures are evaluated, whereas the review of damage assessment of this type of structures is given in [8]. The relationship between damage indices and damage measures was analysed in [9], and the relationship between damage indices and seismic ground motion intensity during the Taiwan Earthquake of 1999 was considered in [10]. General guidelines related to the characteristic formulas of the damage indices of an RC structure was presented in [11], and a correlation study between the seismic acceleration parameters and damage indices of structures was presented in [12]. Nonlinear static analysis was used for the seismic damage assessment of RC structures in [13], whereas [14] focused on a performance-based seismic evaluation procedure for MRF. One of the first books to cover the seismic design of RC structures is [15], whereas [16, 17] provide more detailed information on RC building structures. Another book [18], which covers both the damage and retrofitting of bridges, is one of the most cited books on the subject. In this regard, the adoption of Federal Emergency Management Agency (FEMA) documents has been extensively studied, with particular attention paid to FEMA 356 [19] and ASCE [20].

The development of performance-based seismic engineering has been significantly influenced by the publication of [21]. A wider analysis of performance-based seismic designs was discussed in [22, 23]. Another study [24] focused on the seismic performance and evaluation of RC frames. The Earthquake Loss Estimation Methodology, proposed by FEMA and presented in [25], is widely used worldwide. In Europe, the most commonly used methodology for earthquake loss estimation is presented in [26]. A next-generation seismic performance assessment methodology for existing buildings, including repair cost and repair time, is considered in [27]. Fragility curves (FC) are used for the damage assessment of a structural system, as discussed in [28], whereas the vulnerability assessment of RC-framed structures considering the effect of structural characteristics is discussed in [29]. The vulnerability and risk evaluation of RC structures were analysed in [30]. EN documents for structures [31–36] are used to design seismically resistant structures. The performance-based seismic assessment of RC MRF is presented in [37, 38] considered an efficient analytical fragility function fitting using dynamic structural analysis.

In nonlinear analyses of RC structures, a theoretical stress–strain model developed by Mander, Priestley, and Park for confined concrete [39] is commonly used. This model allows for the introduction of different stress–strain relations of non-stiffened and stiffened parts in the cross sections and structural elements. Statistical analysis and estimation of the data distribution type are described in [30]. The correlation of structural seismic damage with the fundamental period of vibrations of RC buildings, which is often used in seismic analyses, was analysed in [41]. Another study [42] focused on a structural seismic damage assessment method based on structural dynamic characteristics, whereas the damage-based seismic performance evaluation of RC frames is described in [43]. The effects of degradation on the seismic damage of RC buildings were discussed in [44]. The methodology for applying the damage spectrum as a seismic intensity measure in the endurance time of the MRF was presented in [45]. The damage capacity of RC structures using a performance-based analysis was the subject of [46]. The performance evaluation and damage assessment of buildings subjected to seismic loading were discussed in [47]. The development of seismic fragility surfaces for RC buildings by means of a nonlinear time-history analysis was presented in [48], which can be useful in a comparative analysis of the results obtained by different nonlinear analysis methods.

A review of the seismic vulnerability assessment of RC structures is provided in [49], whereas [50] focuses on proposing, comparing, and discussing methodologies for seismic vulnerability assessment indices for buildings at collapse limit states. In [51], the results of a comparative study of building seismic vulnerability assessment methods were analysed. The assessment of the seismic vulnerability of RC-frame buildings is discussed in [52], whereas the vulnerability of buildings in Australia is described in [53]. In [54], the N2 method for the damage estimation of MDOF systems under seismic conditions was evaluated. The main construction systems applied in China and Europe were analysed in [55]. The post-earthquake damage evaluation for RC buildings based on residual seismic capacity is discussed in [56, 57] evaluates the analytical fragility and damage-to-loss models for RC buildings.

In [58], the ATC-58-2 project summarised the development of next-generation performance-based design criteria related to new and existing buildings. A seismic vulnerability evaluation of existing RC buildings was considered in [59]. The vulnerability and fragility of an RC-frame building, with the application of nonlinear time history analysis, was analysed in [60]. In [61], the seismic risk assessment of buildings was discussed, and [62] proposed a mechanistic seismic damage model for RC using a damage index (DI) evaluation formula as a linear combination of plastic deformation and energy distribution. In [63], progress was made in DI by directly modifying the Park–Ang model by eliminating insufficiencies related to the physical meaning of DI. In the seismic response analysis of the building in this study, databases [64, 65] were used, and the methodology proposed in [66] was used for the selection and scaling of [67, 68]. The assessment of the Park–Ang DI for performance levels of RC MRF is presented in [69], whereas the seismic damage assessment of RC structures using nonlinear static analyses is discussed in [70]. Another study [71] analysed the seismic fragility assessment for RC high-rise buildings in the Southern Euro-Mediterranean zone, and [72] used the seismic DI for the classification of structural damage. The modification of the Park–Ang DI to accommodate the effect of aftershocks on RC Structures was discussed more widely in [73], whereas the estimation of the Park–Ang DI for planar multistorey frames using equivalent single-degree systems was analysed in [74]. In [75], the effects of seismic loading patterns on the height-wise distribution of drifts were studied, and in [76], the results of a comparative seismic risk assessment of existing RC buildings were presented. The results of a broader analysis of the FC of existing RC buildings based on specific structural performance levels were presented in [77].

The methodology for developing a seismic vulnerability index for RC buildings based on nonlinear parametric analysis was the subject of [78], whereas an assessment of the vulnerability curves for RC structures using the vulnerability index method is presented in [79]. In [80], a review of seismic vulnerability assessment methodologies was presented, whereas [81] focuses on developing a uniform seismic vulnerability framework for RC buildings. Finally, [82] explored the performance evaluation of RC frame–wall structures using fragility analysis, which is beyond the scope of the constructive systems discussed in this paper and requires further research.

This study aims to analyse the seismic response of an RC building using nonlinear static analysis (NSA) and nonlinear dynamic analysis (NDA) methods. The purpose of this study was to determine the DI using the parameters obtained through NSA and NDA using a software package [83]. The obtained DI values were compared through fragility and vulnerability assessments, and the functions were calculated for each damage state. Two methods were used to obtain the fragility and vulnerability curves. In the first method, the curves were fitted based on the probability of exceedance (PoE) of the damage state. In the second method, the curves were calculated through linear regression analysis; the results obtained using these two methods were compared. The focus of this study is to determine the likelihood of the results obtained using four different DI models: the Park–Ang model using both NSA and NDA results (M1), modified Park–Ang model using both NSA and NDA results (M2), Park–Ang model using NSA results (M3), and modified Park–Ang DI model using NSA results (M4). One of the objectives was to obtain the values of DI, fragility, and vulnerability assessment results using only NSA parameters and compare them with the results obtained using both the NDA and NSA methods. This approach simplifies the calculation process and reduces the time required for the determination of DI and assessment of fragility and vulnerability. The research was conducted on one structural model of an RC-frame building, and it is necessary to investigate the results of this approach using different structural models.

2. Structural modelling and analysis

2.1. Geometric and material properties

The subject of the analysis was an office/residential building frame structural system (Figure 1) with five levels (ground floor + four storeys), as shown in Figure 1. The length of one span in both directions is 4.8 m, which makes the total length of the building 19.2 m in both the directions; height of the first story is 3.6 m, and the heights of the other stories are 3.2 m, which makes the total height of the building 16.4 m. All ground floor vertical elements are fixed at the bottom level of the structure. The building model, which is described in detail in [60], was calculated using ETABS [83]. The properties of the cross-sections are shown in Figure 2.

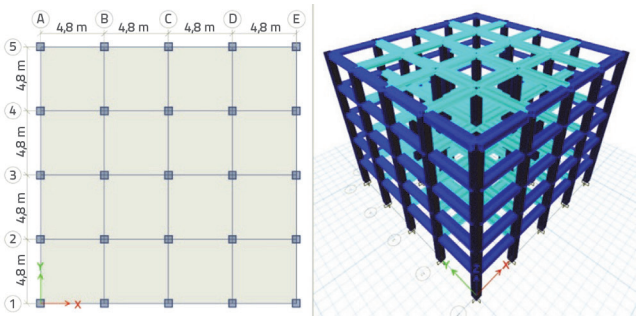

Figure 1. Building plan (left); numerical model (right), according [60]

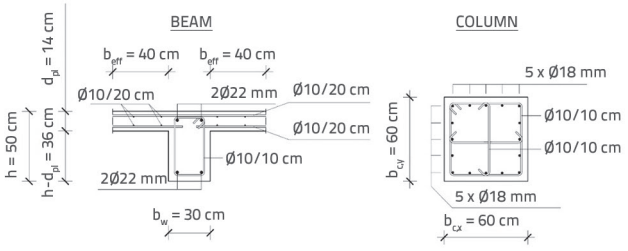

Figure 2. Geometric properties and reinforcement, according [60]

2.2. Loads and actions and modal analysis

The loads acting on the structure include permanent loads (G_i), variable live loads (Q_i), and seismic loads (S_i). The adopted value of the permanent constant load is g_{pl} = 3.0 kN/m^2, and the load intensity of the variable live load amounts to q = 2.0 kN/m^2 on all floors except the roof, where it amounts to q_R = 1.0 kN/m^2. The self-weight load of the facade elements is equal to g_f = 10.0 kN/m. To calculate the impact of an earthquake on the structure, an elastic response spectrum, type 1, was used for the ground type C, with a PGA of a_g = 0.2·g [60].

Modal analysis was performed to determine the fundamental periods of vibration of the system and its modes. It was established that the system was torsionally rigid and that the translational modes were dominant. Rayleigh viscous (mass–tangent stiffness) proportional damping was used in the NDA [60].

The adopted loads and actions on the structure, as well as the modal analysis, are described in [60]. The fundamental period T_1 was 0.735 s (80.41 % mass) and T_2 was 0.213 s (92.69 % mass in sum).

2.3. Loads and actions and modal analysis

Ten accelerograms (Figure 3 and Table 1) were used to perform the one-directional NDA. These records correspond to soil type C [31]. The main criterion for selecting earthquake records was that the mean of the selected and scaled records should match the elastic response spectrum EN1998-1 [31] used in the analysis. THA data were scaled with a common scale factor F_S = 1.61, which was obtained using the least-squares method.

Scaled accelerograms are used for NDA, with the increment of ΔPGA = 0.1 *g*, in a total scaling factor range of 0.1–1.0 *g*. The entire procedure has been described in detail in [60].

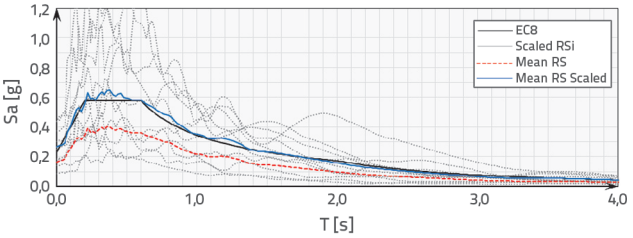

Figure 3. Response spectra and TH data, after [60]

2.4. Model for nonlinear analysis

In the models for the post-elastic analysis, the following assumptions and simplifications were used [60]:

- The calculation includes the effects of the second-order logic (*P*–Δ);
- To describe the nonlinear behaviour of the material, its nonlinear properties are used to describe the behaviours of concrete [35, 39] and reinforcement steel [36, 39].
- The behaviour of RC is described by the Takeda hysteresis model, whereas the kinematic model of hysteresis is used for reinforcement.
- The columns and beams are modelled as confined RC elements with a protective layer of concrete.
- The beams are modelled as "*L*" and "*T*" cross-sections, with the effective width of the RC plate.
- RC plates are modelled as rigid diaphragms.

Table 1. Earthquakes used in NDA

ID br.	Earthquake Location	Earthquake ID (Component/Orientation)	Station ID/Code	Date/Time	M_w	Original PHA [cm/s^2]
EQ01	Spitak, Armenia	213 (Y)	173	07.12.1988. 07:41:24	6.7	179.580
EQ02	Manjil, Western Iran	230 (Y)	189	20.6.1990. 21:00:08	7.4	87.045
EQ03	Umbria Marche, Central Italy	286 (Y)	221	26.9.1997. 09:40:30	6.0	218.340
EQ04	Umbria Marche, Central Italy	286 (Y)	224	26.9.1997. 09:40:30	6.0	106.660
EQ05	Alkion, Greece	559 (X)	214	15.6.1995. 00:15:51	6.5	55.501
EQ06	Düzce, Turkey	497 (Y)	3139	12.11.1999. 16:57:20	7.2	112.320
EQ07	Umbria, Central Italy	EMSC-20161030_0000029 (N-S)	CNE	30.10.2016. 06:40:18	6.5	288.280
EQ08	Emilia-Romagna, Italy	IT-2012-0011 (N-S)	MOG0	29.5.2012. 07:00:02	6.0	167.075
EQ09	Adana, Turkey	TK-1998-0063 (E-W)	0105	27.6.1998. 13:55:53	6.2	271.955
EQ10	Emilia-Romagna, Italy	IT-2012-0011 (N-S)	MIR08	29.5.2012. 07:00:02	6.0	242.970

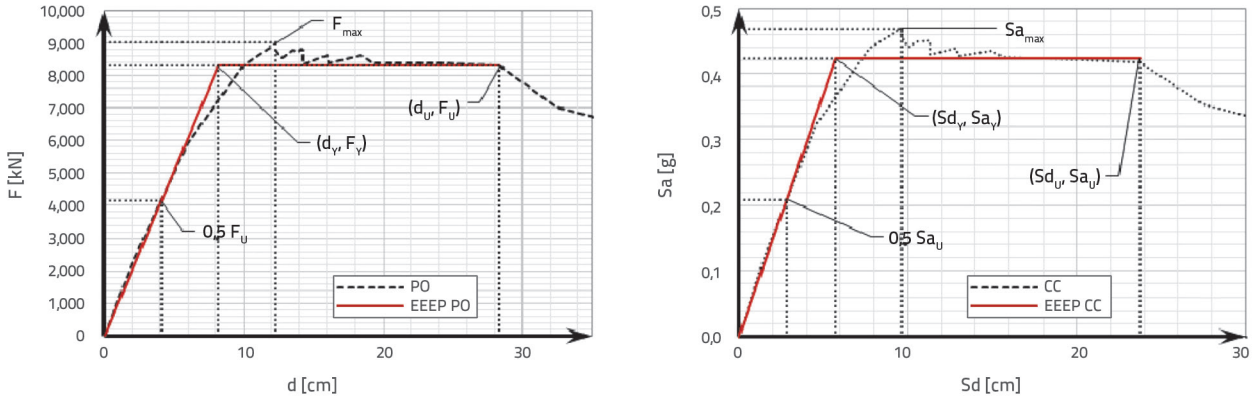

Figure 4. Capacity curve (left) and pushover (right) bilinear approximations, according [60]

3. Nonlinear analysis results

3.1. Nonlinear static analysis

The determination of yielding (d_Y,F_Y) = (8.19 cm, 8283.23 kN), ultimate capacity (d_U,F_U) = (28.39 cm, 8283.23 kN), spectral yielding (Sd_Y,Sa_Y) = (5.72 cm, 0.423 g), and spectral ultimate capacity (Sd_U,Sa_U) = (21.42 cm, 0.423 g) was performed using the EEEP method, as described in detail in [60].

3.2. Damage state performance points

The damage state performance points are determined in the same manner as in [60] through threshold performance points, using DI as a reference parameter. The methods described in [26, 62, 71, 74] were used to calculate the fragility curve.
Four models based on two calculation methods and two methods of analysis were used to calculate the DI values:

- Model 1 (M1): represents the DI calculated based on the method proposed by Park and Ang [62] used in [71]; it is calculated based on the results of the pushover NSA and NDA parameters.

$$DI_{M1} = DI_{PA}^{NDA} = \frac{D_{\max}^{NDA}}{D_u^{NSA}} + \beta \cdot \frac{1}{F_y^{NSA} \cdot D_u} \cdot E_H^{NDA} \quad (1)$$

(if $F_u < F_y$, F_y is replaced by F_u)

- Model 2 (M2): represents the DI calculated based on the modified Park–Ang DI [62] described in [74], and the values were obtained from the results of the pushover NSA and NDA parameters. This model includes the yield displacement value in part of the equation and yielding factor in the relationship between the maximum roof behaviour d_{max} and ultimate roof displacement of the structure, as determined by NSA.

$$DI_{M2} = DI_{MOD}^{NDA} = \frac{D_{\max}^{NDA} - D_y^{NDA}}{D_u^{NSA} - D_y^{NDA}} + \beta \cdot \frac{1}{F_y^{NSA} \cdot D_u} \cdot E_H^{NDA} \quad (2)$$

(if $F_u < F_y$, F_y is replaced by F_u)

- Model 3 (M3) represents the DI calculated based on the method proposed by Park and Ang [62, 71]; it is calculated based only on the results of the pushover NSA.

$$DI_{M3} = DI_{PA}^{NSA} = \frac{d_p^{NSA}}{d_u^{NSA}} + \beta \cdot \frac{1}{a_y^{NSA} \cdot d_u} \cdot E_H^{NSA} \quad (3)$$

(if $F_u < F_y$, F_y is replaced by F_u)

- Model 4 (M4) represents the DI calculated according to the modified Park–Ang DI [62] proposed in [26, 74]; it is calculated based only on the NSA results. This model includes the yield displacement value in part of the equation and yielding factor in the relationship between the maximum roof displacement d_{max} and ultimate roof displacement of the structure, as determined by NSA.

$$DI_{M4} = DI_{MOD}^{NSA} = \frac{d_p^{NSA} - d_y^{NSA}}{d_u^{NSA} - d_y^{NSA}} + \beta \cdot \frac{1}{a_y^{NSA} \cdot d_u} \cdot E_H^{NSA} \quad (4)$$

(if $F_u < F_y$, F_y is replaced by F_u)

where β = 0.15 for RC structures [63], and $D_{\max}^{NDA}$ is the maximum roof displacement under an earthquake, obtained using NDA, based on the THA data; D_p^{NDA} represents the target roof spectral displacement under the same earthquake, but obtained using the corresponding response spectra in NSA. D_u^{NSA} represents the ultimate roof displacement on the bilinear pushover curve, and d_u^{NSA} represents the ultimate roof displacement on the corresponding bilinearised capacity curve; both the values were determined using NSA.

F_y^{NSA} is the yield force on the bilinearised pushover curve, and a_y^{NSA} represents the yield spectral acceleration value on the corresponding bilinearised capacity curve. Both values were determined using NSA; D_y^{NDA} is the first yield displacement when E_h reaches a nonzero value, obtained using the NDA; d_y^{NSA} represents the yield roof displacement on the bilinearised capacity curve obtained using the NSA D_y^{NDA} has a different value for each TH data set and each intensity measure (IM, where IM = PGA); the value of d_y^{NSA} is determined on the bilinearised capacity curve and has a constant value.

E_H^{NDA} is the hysteretic energy absorbed during a seismic action, and it is obtained using NDA and used in M1 and M2.

$$E_H^{NDA} = \int_{E(t=0)}^{E(t=n)} dE \geq 0 \quad (5)$$

with the boundary conditions of [60].

E_H^{NSA} is the hysteretic energy dissipated by damping, which was obtained using the NSA, calculated according to [84], and used in M3 and M4.

$$E_H^{NSA} = 4 \cdot \left(a_y^{NSA} \cdot d_p^{NSA} - a_p^{NSA} \cdot d_y^{NSA} \right) \quad (6)$$

They are obtained, as shown in Figure 5 and has different values for each TH and IM datasets.
The values of the yield displacements (d_y), as shown in Figure 6 (left), were used in the DI assessment based on the results of the NDA. The scheme in Figure 6 (right) represents the procedure for calculating the hysteretic energy for the NSA procedure and DI calculation based on the results.

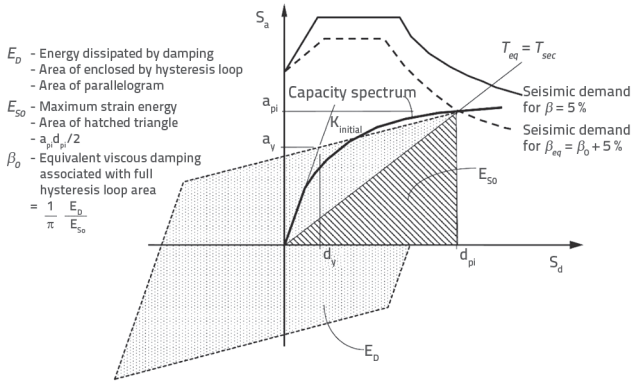

Figure 5. Derivation of hysteretic energy E_H^{NSA}, according [19]

The DI values for all four calculation models are displayed in Figures 7 and 8; they were used for further assessment of the fragility and vulnerability functions.
The DI values for all four calculation models are displayed in Figure 9; they are used for further assessment of the fragility and vulnerability functions.

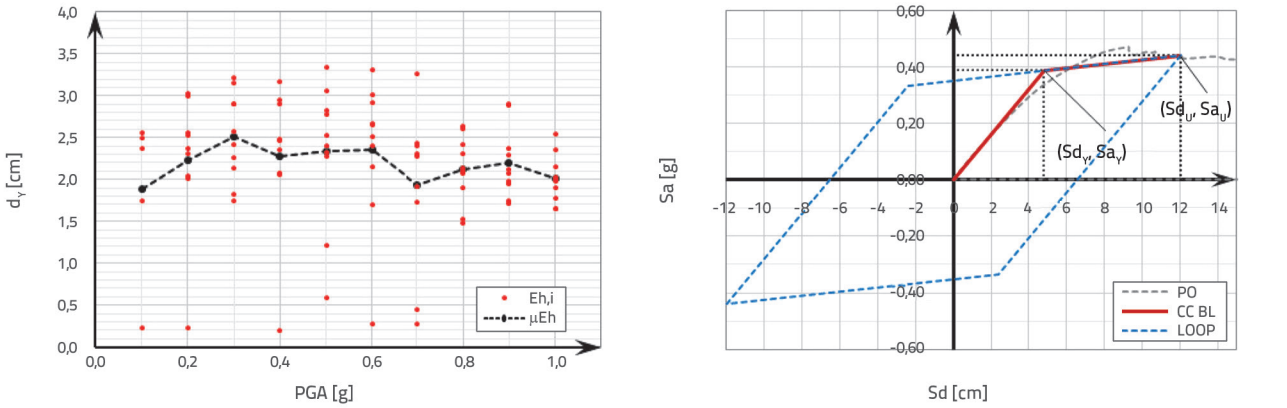

Figure 6. First yield displacement values obtained using NDA (left) and absorbed hysteretic energy calculation method from the pushover results obtained using NSA (right), according [60]

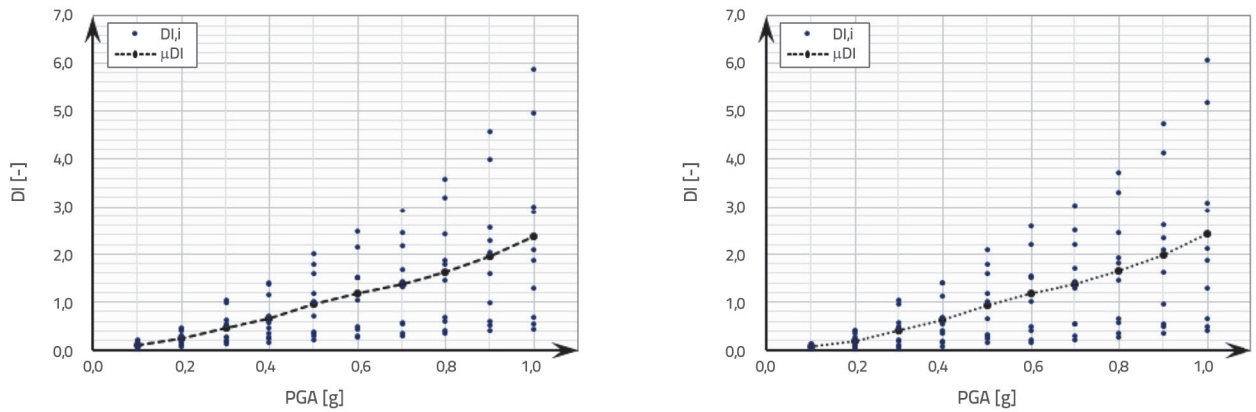

Figure 7. Damage index values for M1 (left) and M2 (right)

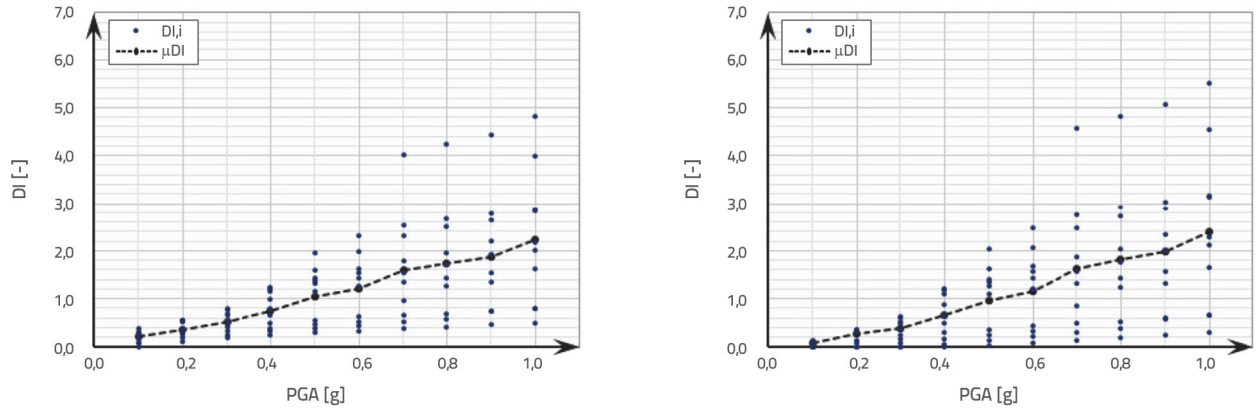

Figure 8. Damage index values for M3 (left) and M4 (right)

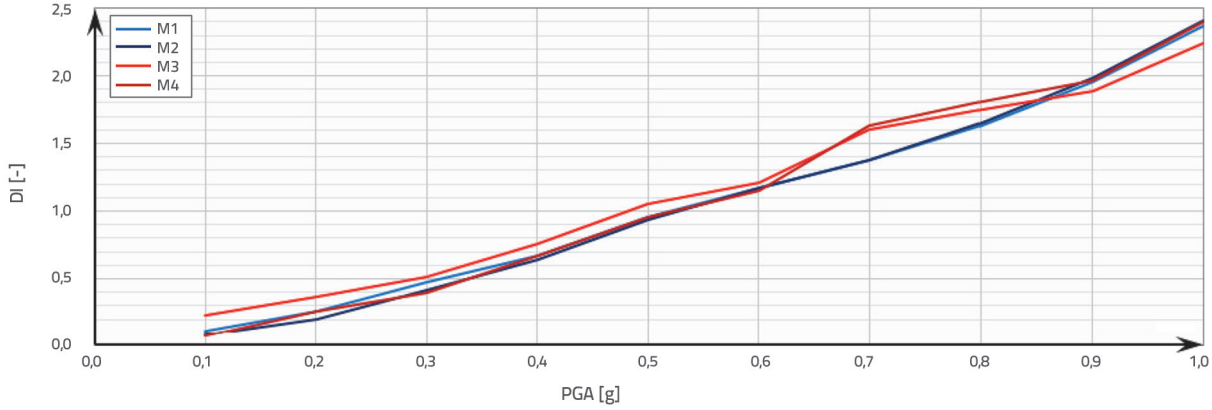

Figure 9. Damage index values for M1–M4

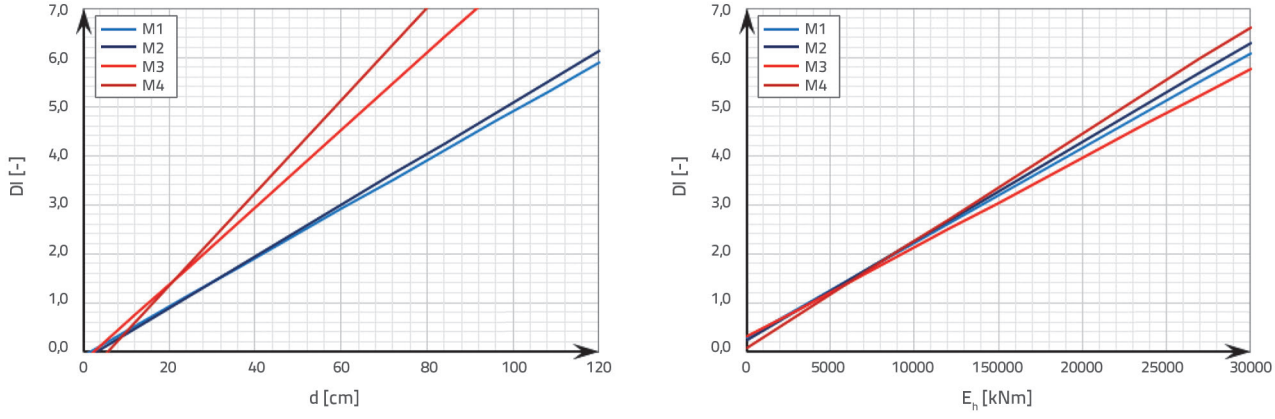

Figure 10. Comparison of d–DI (left) and Eh–DI (right) relationship for M1–M4

Linear regression analysis was performed to determine the relationship between the DI and roof displacement values *d* for all four calculation models. Similarly, a linear regression analysis was performed to determine the relationship between the DI and dissipated energy values, E_h, for all the calculation models. The linear relationships and correlation values are presented in Equation (7). The linear relationships between DI and d and between DI and E_h are shown in Figure 10.

$$DI_{M1} = 0,0497 \cdot d - 0,0720;\ R = 0,9831$$
$$DI_{M1} = 0,000193 \cdot E_h + 0,285479;\ R = 0,9168$$

$$DI_{M2} = 0,0523 \cdot d - 0,1449;\ R = 0,9842$$
$$DI_{M2} = 0,000202 \cdot E_h + 0,233458;\ R = 0,9129$$

$$DI_{M3} = 0,0786 \cdot d - 0,1900;\ R = 0,9980$$
$$DI_{M3} = 0,000182 \cdot E_h + 0,305668;\ R = 0,9947$$

$$DI_{M4} = 0,0941 \cdot d - 0,5126;\ R = 0,9938$$
$$DI_{M4} = 0,000218 \cdot E_h + 0,079639;\ R = 0,9970 \quad (7)$$

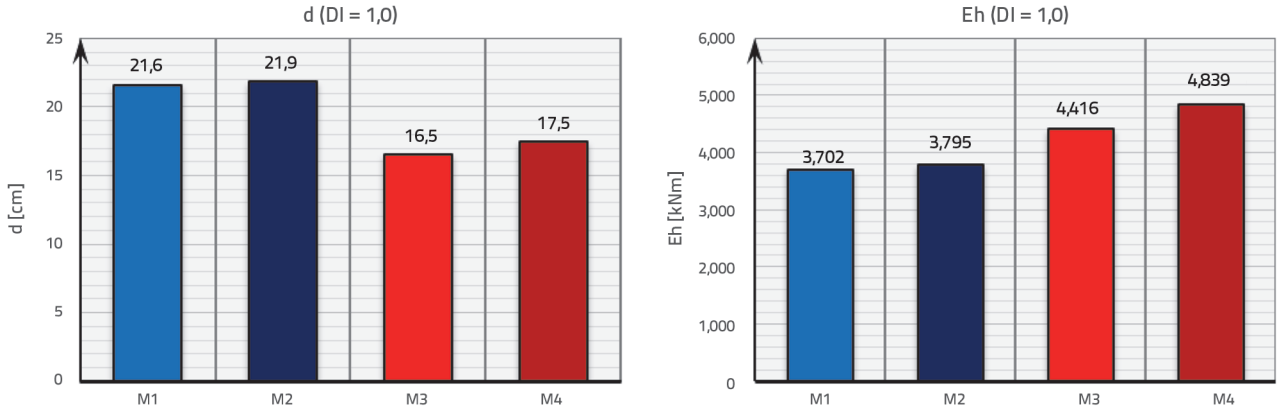

Figure 11. Comparison of d (left) and Eh (right) for DI = 1.0 (M1–M4)

A comparison of the results was performed for DI = 1.0, for which the structure loses its bearing capacity and is in the structural damage state of complete damage (Figure 11).
Although the relation among the functions shown in Figure 11 is not fully described, it can be concluded that using calculation models M1 and M2, based on both NSA and NDA methods, the structure will reach a value of DI = 1.0, with roof displacement values higher than those obtained using calculation models M3 and M4 in the range of 23.2–32.5 % and lower hysteretic energy values in the range of 14.1–23.5 %.

3.3. Statistical analysis of the results

For each PGA and DI distribution, the values fit a lognormal distribution. This implies that the relationship between ln(PGA) and ln(DI) has a normal distribution for each ln(PGA) in the log–log space. Statistical analysis of the results was performed the same way as described in [60].

4. Discussion of the results

4.1. Fragility analysis

The FC and PoE of damage states (DS) was calculated using the expression (8):

$$P_{DS_i/IM_j}\left(\mu^{EDP_i}_{LN,IM_j},\sigma^{EDP_i}_{LN|\,IM_j}\right)=1-\theta\left(\frac{\ln EDP-\mu^{EDP_i}_{LN,IM_j}}{\sigma^{EDP_i}_{LN|\,IM_j}}\right) \quad (8)$$

A more detailed explanation of the calculation process and equation parameters is provided in [60].
Curve fitting (CF) and linear regression (LR) were used to calculate the FC using the analytical cumulative distribution function (CDF) for the lognormal distribution.

$$P_{DS_i/IM}\left(\mu^{IM}_{LN|\,DS_i},\sigma^{IM}_{LN|\,DS_i}\right)=\theta\left|\frac{\ln IM-\mu^{IM}_{LN|\,DS_i}}{\sigma^{IM}_{LN|\,DS_i}}\right| \quad (9)$$

This procedure was described in detail in the paper [60].
The damage state values were defined as slight damage (DI_{SD} = 0.10), moderate damage (DI_{MD} = 0.25), extensive damage (DI_{ED} = 0.40), and complete damage (DI_{CD} = 1.00), according to [74].
The results of the structural analysis used in the CF method for calculating FC and their distributions are shown in Figure 12 (left), whereas the results of the structural analysis used in the LR method for calculating FC and their linear function relationships between IM and EDP are shown in Figure 12 (right).

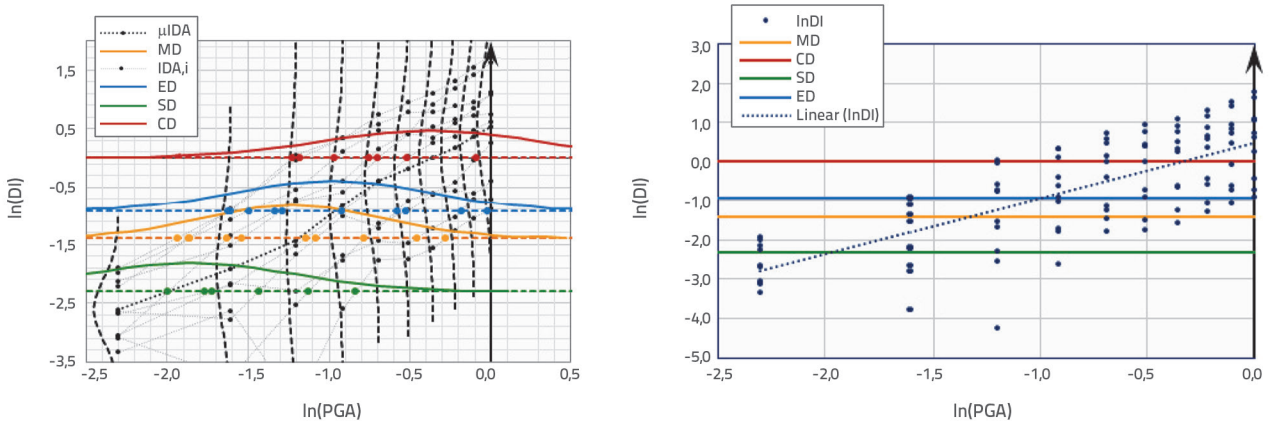

Figure 12. Example of the assessment of PoE of a particular DS for each IM (left) and linear regression method (right) for M2

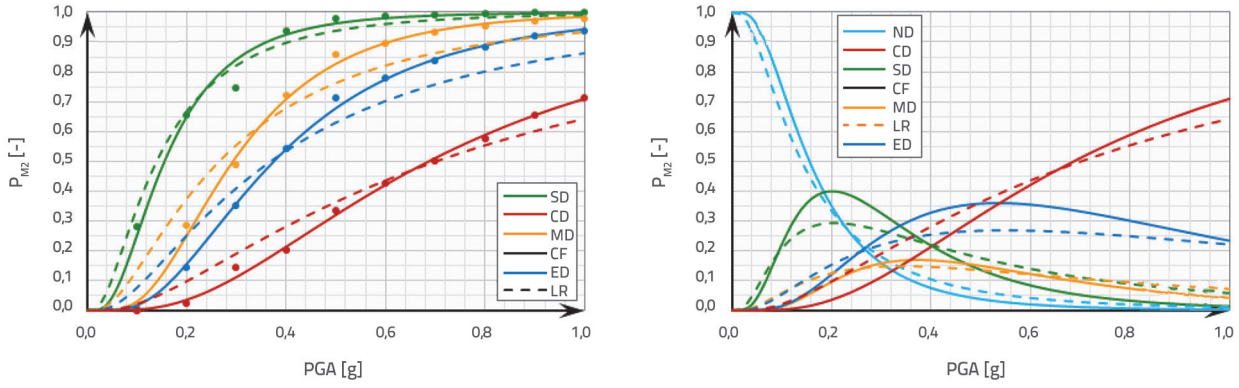

Figure 13. Fragility curves (left) and PDF (right) for M2

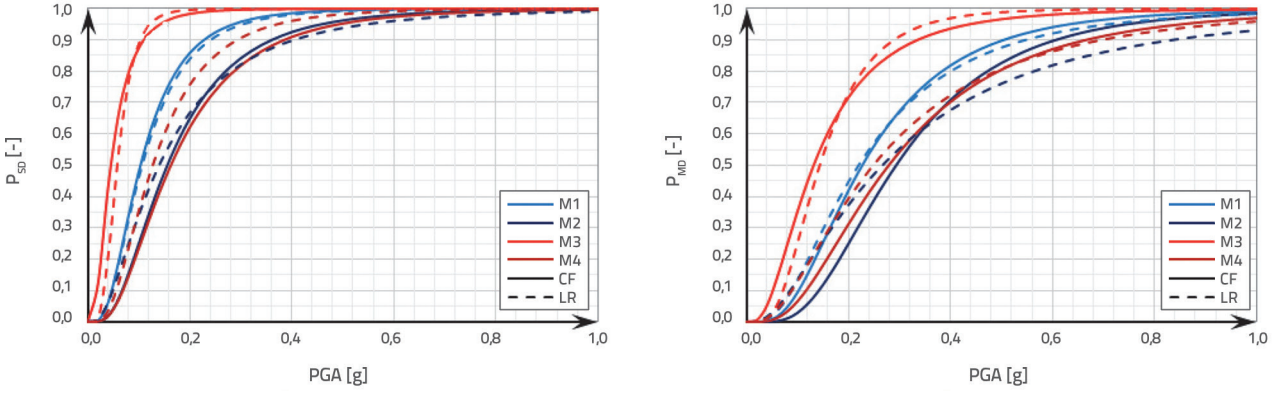

Figure 14. Fragility curves for the occurrence of SD (left) and MD (right) for M1–M4

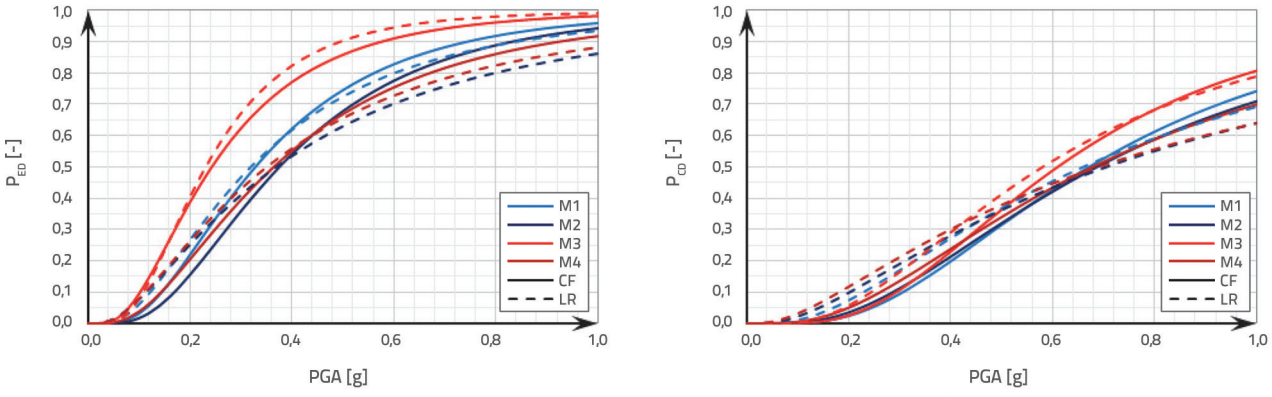

Figure 15. Fragility curves for the occurrence of ED (left) and CD (right) for M1–M4

Based on the obtained results, the FC and probability density functions (PDFs) were calculated. An example of M2 is shown in Figure 13 for all four models of DI determination.

The PDFs for the occurrence of different damage states were calculated using the equations described in [2, 38]:

$$P_{DS0} = 1 - P_{DS1}[IM_j, \mu_{LN|DS1}, \sigma_{LN|DS1}]$$

$$P_{DS1} = P_{DS1}[IM_j, \mu_{LN|DS1}, \sigma_{LN|DS1}] - P_{DS1+1}[IM_j, \mu_{LN|DS1+1}, \sigma_{LN|DSi+1}] \quad (10)$$

$$P_{DSn} = P_{DSn}[IM_j, \mu_{LN|DSn}, \sigma_{LN|DSn}]$$

After calculating the FC, the structural responses of the RC building were compared for each damage state (Figures 14 and 15). It is evident that models M1–M4 differ from each other for a certain value, and a difference based on the analysis approach and curve calculation method exists. However, for both fragility curve calculation methods, the results obtained using M2 model with the combined (NSA and NDA) approach are very similar to those obtained using M4 model, where the DI values and parameters were calculated using only the NSA method. Both models represent the modified Park–Ang DI calculation models.

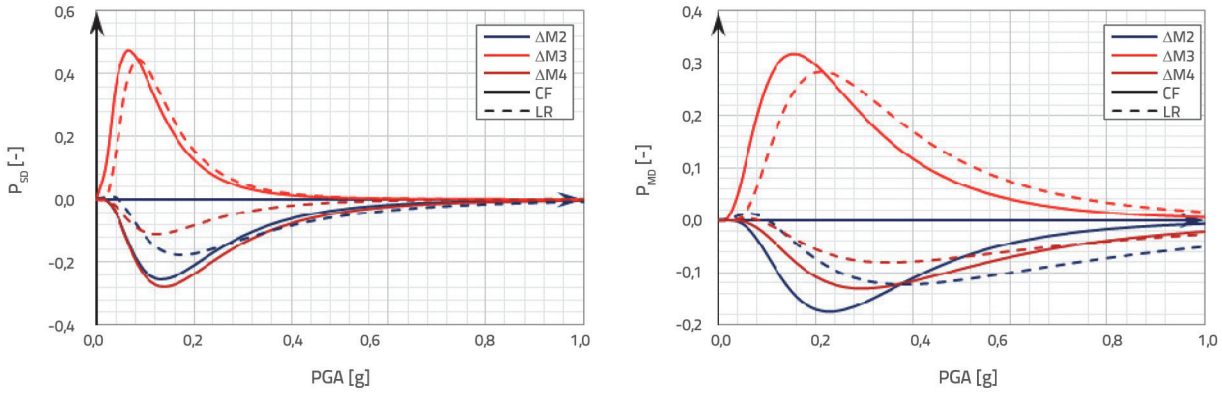

Figure 16. Difference between fragility curves for referent model M1, for SD (left) and MD (right)

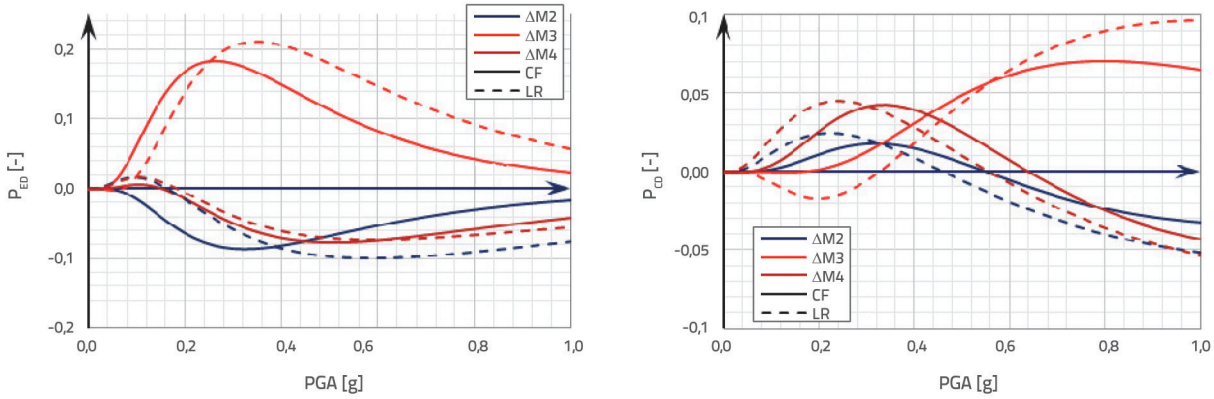

Figure 17. Difference between fragility curves for referent model M1, for ED (left) and CD (right)

For functions related to cumulative distribution functions (CDF) or FC, the conclusions related to the relationships between PDFs are the same as those mentioned for the CDF.

Four calculation models M1–M4 were used for a comparative analysis of the results. Model M1 was selected as the comparative reference model in the first iteration. The differences between the FC (Figures 16 and 17) calculated using all the models were calculated using the following equations:

$$\Delta P_{DI|\,IM_j}^{Mi} = P_{DS_i|IM_j}^{M_i} - P_{DS_i|\,IM_j}^{M_{ref}} \tag{11}$$

$$\Delta MDF_{DI|\,IM_j}^{M_i} = MDF_{DS_i|\,IM_j}^{M_i} - MDF_{DS_i|\,IM_j}^{M_{ref}} \tag{12}$$

index DS_i represents a particular damage state, M_j is the value of the intensity measure, DI represents the DI, MDF is the mean damage factor, and M_i and M_{ref} are the analysed and reference models, respectively.

M2 and M4 values were closer to M1 than to M3. It is evident that, as previously stated, the smallest difference was obtained between M2 and M4; these models should be further compared and analysed.

4.2. Vulnerability analysis

The vulnerability curves were calculated according to the method described in [60]. The vulnerability curves were calculated based on the fragility results according to the equation and process described in [3]:

$$E(C|IM) = \sum_{i=0}^{n} E(C|DS_i) \cdot P(DS_i|IM) \tag{13}$$

where n is the number of considered DS DS (DS_i), $P(DS_i|IM)$ is the damage probability, and are the cumulative distribution of cost (or loss) according to [3]. The values of $E(C|DS_i)$ are adopted from [5]. The results are compared and displayed in Figure 18.

Because the vulnerability curves are calculated based on the fragility parameters, the relationship between the results will

Table 2. Damage factor functions of building typology according to [3]

Damage scale	E(C|DS$_i$)			
Damage state	Slight	Moderate	Extensive	Complete
	2 %	10 %	50 %	100 %

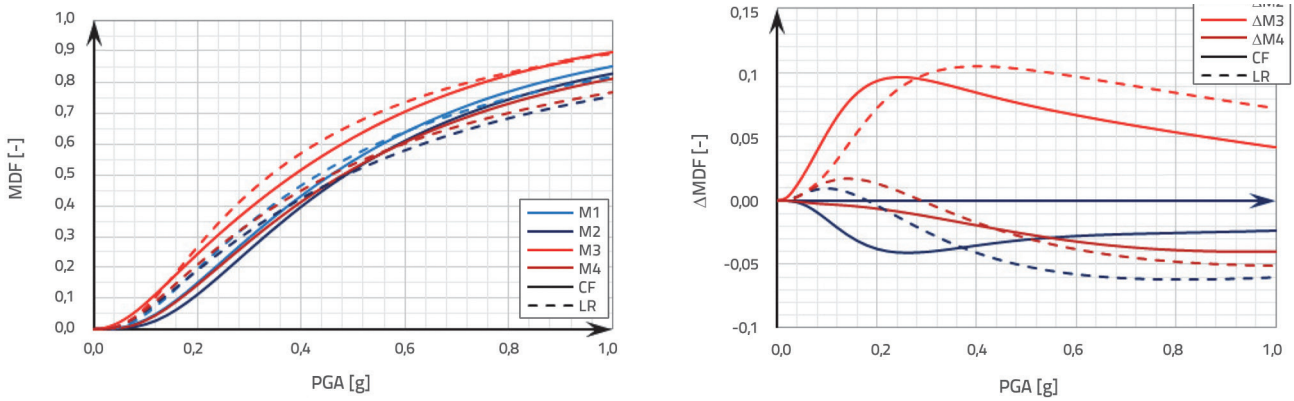

Figure 18. Vulnerability curves for M1–M4 (left) and difference between vulnerability curves for referent model M1 (right)

be the same as in the case of the fragility assessment, which implies that M2 and M4 values are closer to M1 than M3. It is also evident that, as previously stated, the smallest difference is between M2 and M4, and that these models should be further compared and analysed.

4.3. Comparative analysis of the results

Comparing the fragility and vulnerability curves through a numerical comparison of the models for each PGA is inconvenient because it is already represented through visual comparison in Figures 16–18; it describes the differences between the results obtained using different DI models and different methods of structural response analysis. The differences between the models and methods are shown in Figures 19 and 20 for the design with PGA = 0.2 *g*. However, no clear pattern can be observed in Figures 19 and 20, except a clear deviation in M3 compared with the other models.

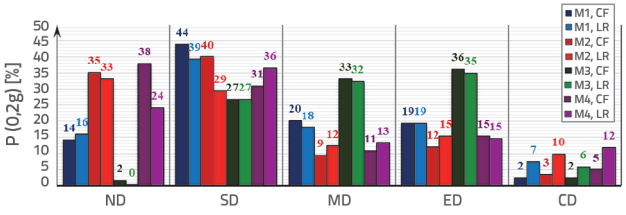

Figure 19. PoE of particular DS for M1–M4 for PGA = 0.2 g

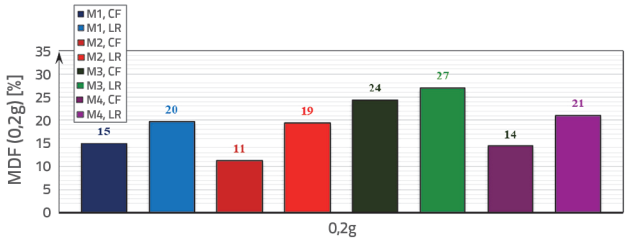

Figure 20. PoE of particular MDF for M1–M4 for PGA = 0.2 g

No clear pattern can be observed from Figures 21–25, except a clear deviation in M3 compared with the other models. In further analysis, the results of fragility and vulnerability will be observed using only two models: the modified Park–Ang DI model calculated using NSA and NDA parameters (M2), which should give the most accurate input in seismic response of the structure, because it includes maximum roof displacements under earthquake D_{max}^{NDA}, obtained using NDA, ultimate roof displacement on bilinearised pushover curve D_u^{NSA}, yield force on bilinearised pushover curve F_y^{NSA}, first yield displacement D_y^{NDA}, and absorbed hysteretic energy during the earthquake E_H^{NDA}; the model with parameters, which are corresponding to the ones given in M2 but obtained only using NSA (M4). These two models had the most similar results obtained using either the CF or LR calculation methods. Model M2 was selected as the reference comparison model.

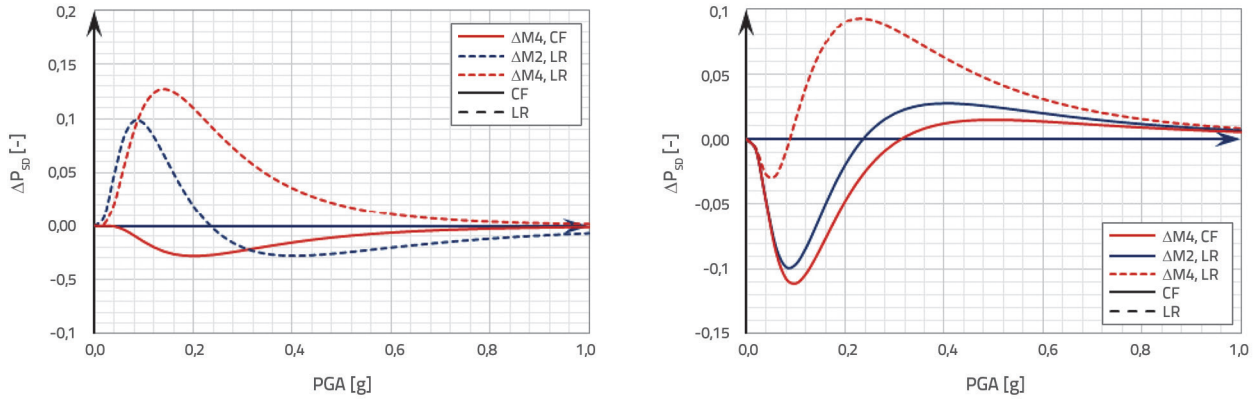

Figure 21. Difference between fragility curves for referent model $M2^{CF}$ (left) and $M2^{LR}$ (right) for SD

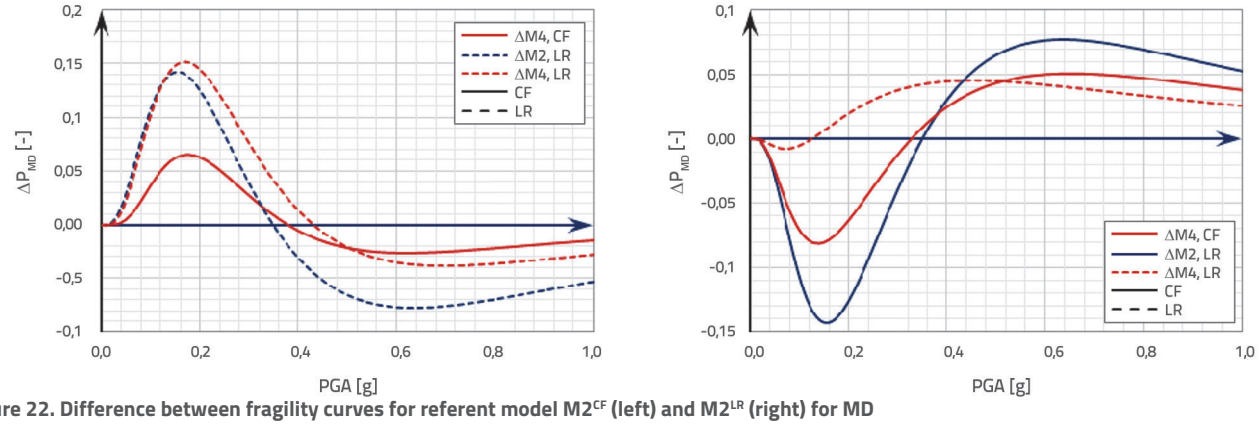

Figure 22. Difference between fragility curves for referent model M2^{CF} (left) and M2^{LR} (right) for MD

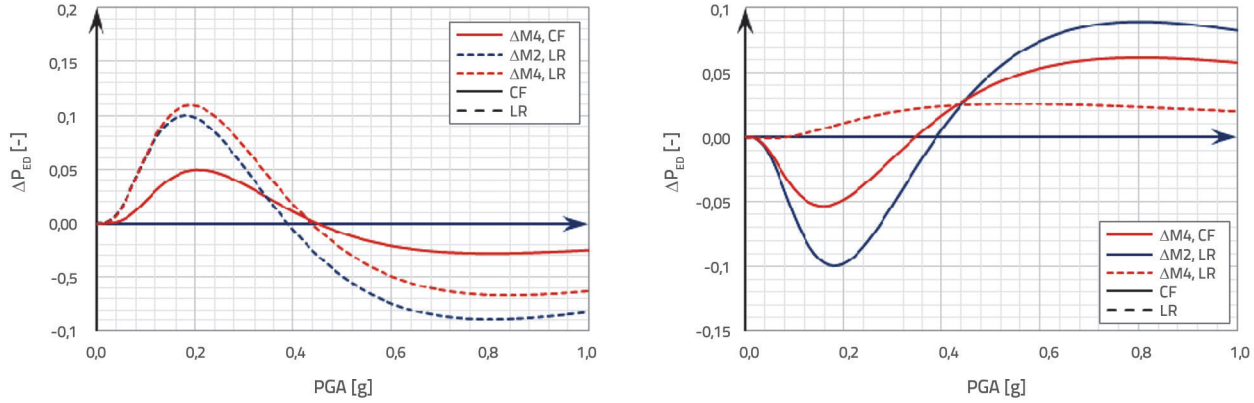

Figure 23. Difference between fragility curves for referent model M2^{CF} (left) and M2^{LR} (right) for ED

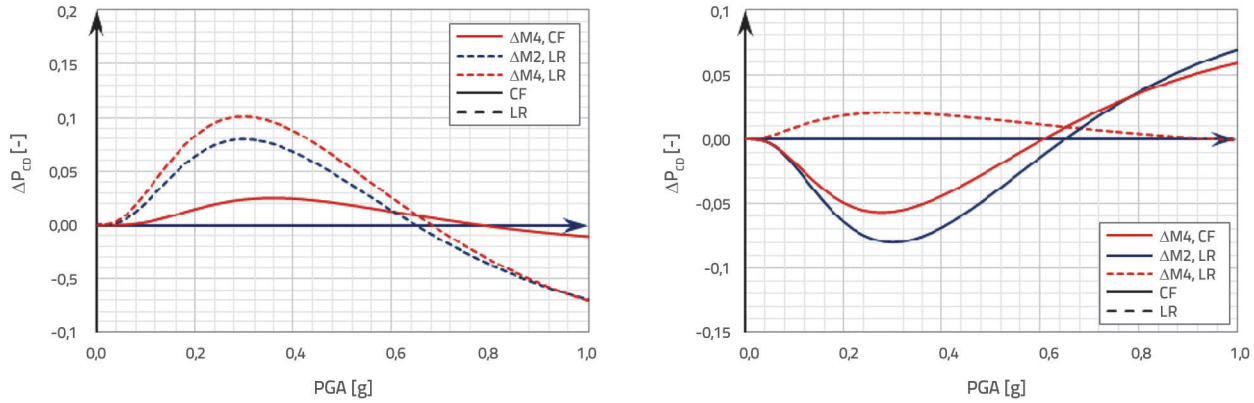

Figure 24. Difference between fragility curves for referent model M2^{CF} (left) and M2^{LR} (right) for CD

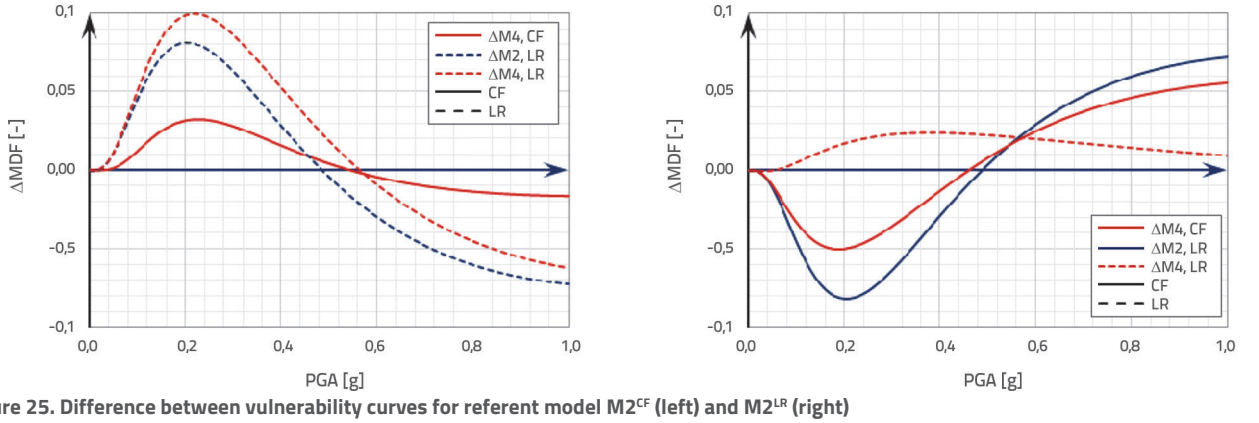

Figure 25. Difference between vulnerability curves for referent model M2^{CF} (left) and M2^{LR} (right)

If $M2^{CF}$ is selected as the reference model, the smallest deviations in the value of the PoE for all DS and in vulnerability analysis will be in the case of $M4^{CF}$ model, followed by models $M2^{LR}$ and $M4^{LR}$, as anticipated. The ranges between the deviations are shown in Figures 21–25 (left). When $M2^{LR}$ is selected as the referent model, the smallest deviations in the value of the PoE for all DS and in vulnerability analysis will be in the case of $M4^{LR}$ model, followed by models $M2^{CF}$ and $M4^{CF}$, as anticipated. The ranges between the deviations are shown in Figures 21–25 (right).

The results deviate in the range of -2.80 % to +6.52 % in fragility and in the range of -1.64 % to +3.24 % in vulnerability analysis when $M4^{CF}$ is compared with the reference model $M2^{CF}$, which is the case where DI values are obtained by NSA and NDA ($M2^{CF}$) and only NSA ($M4^{CF}$), using the curve fitting method for the derivation of FC based on the PoE of the DS analysis. (Figure 26)

In the case of the results obtained using the linear regression method for the derivation of FC, compared with the reference model $M2^{CF}$, the difference between the results is larger, ranging from -8.93 % to +14.27 % in fragility and from -7.21 % to +8.17 % in the vulnerability analysis for $M2^{LR}$ and from -7.07 % to +15.14 % in fragility and from -6.25 % to +10.00 % in the vulnerability analysis for $M4^{LR}$ (Figure 26).

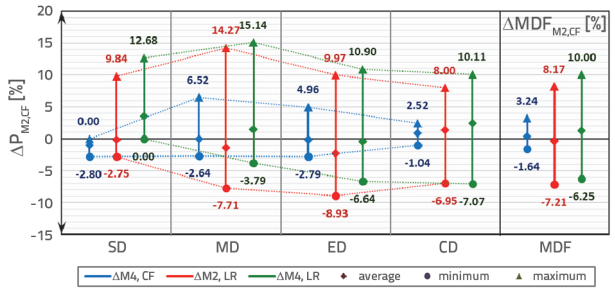

Figure 26. Maximum and minimum difference between fragility curves for referent model $M2^{CF}$

The results deviate in the range of -2.84 % to +9.27 % in fragility and in the range of -0.04 % to +2.40 % in the vulnerability analysis, when $M4^{LR}$ is compared with the reference model $M2^{LR}$ using the linear regression method for the derivation of FC based on the PoE of DS analysis (Figure 27).

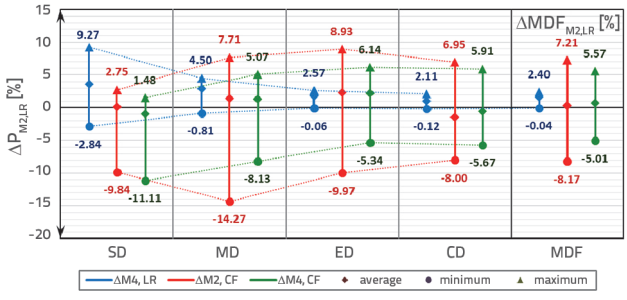

Figure 27. Maximum and minimum difference between fragility curves for referent model $M2^{LR}$

In the case of the results obtained using the curve fitting method for the derivation of FC, compared with the reference $M2^{LR}$ model, the difference between the results is larger, ranging from -14.27 % to +8.93 % in fragility and from -8.17 % to +7.21 % in the vulnerability analysis for $M2^{LR}$ and from -11.11 % to +6.14 % in fragility and from -5.01 % to +5.57 % in the vulnerability analysis for $M4^{LR}$. (Figure 27)

5. Conclusion

This paper presents the calculation and analysis of the DI, fragility, and vulnerability assessment for a 5-storey RC frame structure selected for the case study. Four calculation models (M1–M4) were used to compute DI, and the values were obtained based on the NSA and NDA results. Two methods were utilised to obtain the FC: the fragility curve fitting method, which is based on the calculation of the probability of exceedance of the corresponding damage states and linear regression, wherein a linear relationship in the log–log space is established between the DI and PGA values. The vulnerability curves were determined based on the results of the fragility curve assessment and probability of exceedance of the corresponding damage states as a function of the mean damage factor. These analyses provided the basis for subsequent comparative analyses. Finally, recommendations and conclusions are provided based on the results.

Regarding the approximated DI–roof displacement linear relationships, it can be inferred that models M1 and M2 (based on the NSA and NDA methods) will yield lower DI values for the same roof displacement values compared with models M3 and M4 (based on the NSA), provided that the values of DI_{M3} = 0.12 and DI_{M4} = 0.32 are reached. This implies that after the initial formation of a lower degree of damage, the structure will exhibit a higher degree of damage for lower displacement values if M3 and M4 are used as opposed to M1 and M2. The calculations using M1 and M2 provided a less conservative relationship between the DI and roof displacements for higher degrees of damage. Furthermore, the relationship between the dissipated hysteretic energy and DI was similar in all the models. The results of the DI values and aforementioned relationships are presented in the form of the DI–PGA relationship, and the values of the DI related to the PGA are comparable for all four models. However, when using M3 and M4 (models based on the NSA), the DI of the building was slightly higher or more conservative for most PGA values.

The results of the fragility curve calculation indicate slight variations in the results for all models at a particular value, and a minor difference based on the analysis approach and curve calculation method is observed. However, the results obtained using M2 model, which combines NSA and NDA, are very similar to the results obtained from M4 model, which uses only the NSA method for both fragility curve calculation methods. Both models used the modified Park–Ang DI calculation models.

When the differences between the derived fragility and vulnerability curves were analysed, the results showed that the smallest difference existed between M2 and M4 models, and there was a clear deviation in M3, and then M1, compared with those models. The great similarity between the results obtained using M2 and M4 was established by applying either the CF or LR method for the calculation of the vulnerability curves.

The results suggest that M4 model, which solely employs NSA for DI calculation, can be used to simplify the procedure described by M2 model, which employs both NDA and NSA. The procedures of M4 model are less complex and less time-consuming than those of M2 model; it also satisfies the accuracy requirements of engineering practice. Therefore, the methodologies for the DI, fragility, and vulnerability assessment applied in this study can be generally extended to different types of buildings.

Acknowledgements

This work was supported by the Ministry of Education, Science, and Technological Development of the Republic of Serbia (Contract no 451-03-80/2022-01/1 from 19.12.2022.).

REFERENCES

[1] Sfahani, M.G., Guan, H., Loo, Y.C.: Seismic Reliability and Risk Assessment of Structures Based on Fragility Analysis - A Review, Adv. Struct. Engl., 18 (2015), pp. 1653–1669

[2] Porter, K.A.: Beginner's Guide to Fragility, Vulnerability and Risk, University of Colorado Boulder, Boulder, CO, USA, 2015., DOI:10.1007/978-3-642-35344-4_256.

[3] D'Ayala, D., Meslem, A., Vamvatsikos, D., Porter, K., Rossetto, T., Silva, V.: Guidelines for Analytical Vulnerability Assessment of Low/Mid-Rise Buildings, GEM Technical Report 2015-08 V1.0.0, 2014., https://doi.org/10.13117/GEM.VULN-MOD.TR2014.12.

[4] Korkmaz, K.A.: Evaluation of seismic fragility analysis, Proceedings of the 14th World Conf. on Earth. Engl., China, 2008.

[5] Moussa, A., Christou, P., Kyriakides, N.: The developments of the analytical fragility methods in seismic risk assessment-A review, Journal of Sustainable Architecture and Civil Engineering, 3 (2016) 16, pp. 70-81

[6] Ggadigone, V.S., Takkalaki, S.R., Patil, V.A.: Seismic assessment of reinforced concrete framed structures, Intern. J. on Recent and Inov. Trends in Comp. and CC, 6 (2016) 5, pp. 262-267.

[7] Kappos, A.J.: Seismic damage indices for RC buildings: evaluation of concepts and procedures, Progress of structural engineering materials, 1 (1997) 1, pp. 78-87

[8] Makhloof, D.A., Ibrahim, A.R., Ren, X.: Damage Assessment of Reinforced Concrete Structures through Damage Indices: A State-of-the-Art Review, CMES-Computer Modeling in Engl. & Sciences, 128 (2021) 3, pp. 849–874

[9] Cosenza, E., Manfredy, G.: Damage indices and damage measures, Prog. Struct. Engl. Mater., (2000) 2, pp. 50-59

[10] Miyakoshi, J., Hayashi, Y.: Correlation of Building Damage with Indices of Seismic Ground Motion Intensity During the 1999 Chi-Chi Taiwan Earthquake, Proceedings of the International Workshop on Annual Commemoration of Chi-Chi Earthquake, Taipei, Taiwan, 2000.

[11] Sadeghi, K., Angın, M.M.: Characteristic Formulas of Damage Indices for Reinforced Concrete Structures: A General Guideline, Academic Research International, 3 (2018) 9.

[12] Elenas, A., Meskouris, K.: Correlation study between seismic acceleration parameters and damage indices of structures, Engineering Structures, 23 (2001) 6, pp. 698-704

[13] Zemeeruddin, M., Saleemuddin, K.K.M., Sangle, K.K.: Seizmic damage assessment of RC structure using non-linear static analysis, KSCE Journal of Civil Engineering, 21 (2017), pp. 119-1

[14] Zemeeruddin, M., Sangle, K.K.: Damage assessment of RC moment resisting frames using performance/based seismic evaluation procedure, J. King Saud Univ.-Engl. Sci., 33 (2021), pp. 227–239

[15] Park, R., Paulay, T.: Reinforced Concrete Structures, John Wiley & Sons, New York, USA, 1975.

[16] Paulay, T., Priestley, M.J.N.: Seismic Design of Reinforced Concrete and Masonry Buildings, John Wiley & Sons, New York, USA, 1992., pp. 767

[17] Fardis, M.N.: Seismic Design, Assessment and Retrofitting of Concrete Buildings, Based on EN-Eurocode 8; Geotechnical and Earthquake Engineering, Springer, 8 (2009), pp. 743

[18] Priestley, M.J.N., Seible, F., Calvi, G.M.S.: Seismic Design and Retrofit of Bridges, John Wiley & Sons, New York, USA, 1996.

[19] ASCE: FEMA356: Prestandard and Commentary for the Seismic Rehabilitation of Buildings, USA, 2000.

[20] ASCE: Seismic Evaluation of Buildings, American Society of Civil Engineers, Reston, VA, 2006., pp. 41-13

[21] Structural Engineers Association of California: SEAOC Vision 2000 Committee: Performance-based Seismic Engineering, Sacramento, CA, USA, 1995.

[22] Priestley, M.J.N.: Performance Based Seismic Design, Proceedings of the 12th World Conference on Earthquake Engineering, Auckland, New Zealand, 2000.

[23] Krawinkler, H.: Challenges and Progress in Performance-Based Earthquake Engineering, Proceedings of the International Seminar on Seismic Engineering for Tomorrow-In Honor of Professor Hiroshi Akiyama, Tokyo, Japan, 1999.

[24] Hastemoglu, H.: Seismic performance evaluation of reinforced concrete frames, IOSR J. of Mechanical and Civil Engl., 12 (2015) 5, pp. 123-131

[25] Hazus®-MH 2.1.: Earthquake Loss Estimation Methodology, Advanced Engineering Building Module (AEBM), Technical and User's Manual, Department of Homeland Security, FEMA, Mitigation Division, Washington, DC, USA, 2009.

[26] Milutinović, Z.V., Trendafiloski, G.S.: RISK-UE: An advanced approach to earthquake risk scenarios with applications to different European towns, Contract: EVK4-CT-2000-00014, WP4 Vulnerability of Current Buildings, pp. 110, http://www.civil.ist.utl.pt/~mlopes/conteudos/DamageStates/Risk%20UE %20WP04_Vulnerability.pdf, 1.1.2021.

[27] Federal Emergency Management Agency: FEMA P-58 Next-Generation Seismic Performance Assessment Methodology for Buildings, Volume 1 - Methodology, Report FEMA P-58-1, Washington, D.C., 2018.

[28] Borele, S.V., Datta, D.: Damage Assessment of Structural System Using Fragility Curves, J. Civ. Engl. Environ. Technol., (2015) 2, pp. 72–76

[29] Olteanu, I., Barbat, A.H., Budescu, M.: Vulnerability Assessment of Reinforced Concrete Framed Structures Considering the Effect of Structural Characteristics, Open Civ. Engl. J., (2015) 9, pp. 321–329

[30] Olteanu, I., Vargas, Y.F., Barbat, A.H., Budescu, M., Pujades, L.G.: Vulnerability and Risk Evaluation for a Reinforced Concrete Frame, Bull. Polytech. Inst. Iasi., 57 (2011), pp. 59–60

[31] European Committee for Standardization (CEN): EN1998-Part 1, Eurocode 8: Design of Structures for Earthquake Resistance-Part 1: General Rules, Seismic Actions and Rules for Buildings, Brussels, Belgium, 2004.

[32] European Committee for Standardization (CEN): EN1998-Part 3, Eurocode 8: Design of Structures for Earthquake Resistance-Part 3: Assessment and Retrofitting of Buildings, Brussels, 2004.

[33] European Committee for Standardization (CEN): EN 1990. ICS 91.010.30, Basis of Structural Design, Brussels, Belgium, 2005.

[34] European Committee for Standardization (CEN): EN1991, Eurocode 1: Actions on Structures-Part 1-1: General Actions-Densities, Self-weight, Imposed Loads for Buildings, Brussels, 2002.

[35] European Committee for Standardization (CEN): EN1992-Part 1, Eurocode 2: Design of Concrete Structures-Part 1-1: General Rules and Rules for Buildings, Brussels, Belgium, 2004.

[36] European Committee for Standardization (CEN): EN1998-Part 2, Eurocode 8: Design of Structures for Earthquake Resistance-Part 2: Bridges, Brussels, Belgium, 2005.

[37] Zemeeruddin, M., Sangle, K.K.: Performance-based seismic assessment of RC moment resisting frames, J. King Saud. Univ. Engl. Sci., 33 (2021), pp. 153–165

[38] Baker, J.W.: Efficient analytical fragility function fitting using dynamic structural analysis, Earthq. Spectra, 31 (2015), pp. 579–599

[39] Mander, J., Priestley, M., Park, R.: Theoretical Stress-Strain Model for Confined Concrete, J. Struct. Engl., 114 (1988), pp. 1804–1825

[40] MathWave Technologies: EasyFit software: Version 5, http://www.mathwave.com, 1.1.2021.

[41] Eleftheriadou, A. K., Karabinis, A. I.: Correlation of Structural Seismic Damage with Fundamental Period of RC Buildings, Open Journal of Civil Engineering, (2013) 3, pp. 45-67

[42] Wang, M., Gao, L., Yang, Z.: Structural seismic damage assessment method based on structural dynamic characteristics, Research Square, 2022.

[43] Ae-Heo, Y., Kunnath, K.: Damage-based seismic performance evaluation of reinforced concrete frames, International J. of Concrete Structures and Materials, 7 (2013) 3, pp. 175-183

[44] Khoshrafter, A., Albbasnia, R., Raof, F.F.: The effect of degradation on seismic damage of RC buildings, Advances in Environmental Biology,75 (2013) 5, pp. 861-867

[45] Maleki-Amin, M.J., Estekanchi, H.E.: Application of damage spectra as seismic intensity measures in endurance time method for steel moment-resisting frames, Scintia Iranica, 24 (2017) 1, pp. 53-64

[46] Spandana, K., Raju, Y.K., Satyanarayana, G.V.V., Manchalwar, A.: Damage capacity on RC structures using performance based analysis, E3S Web of Conferences 309, No. 01203, 2012.

[47] Chandrasekaram, S., Serino, G., Gupta, V.: Performance evaluation and damage assessment of buildings subjected to seismic loading, Structures under Shock and Impact X, WIT Transaction on the Built Environment, 98 (2008), pp. 313-322

[48] Seyedi, D.M., Gehl, P., Douglas, J., Davenne, L., Mezher, N., et al.: Development of seismic fragility surfaces for reinforced concrete buildings by means of nonlinear time-history analysis, Earth. Engl. & Struct. Dynamics, 39 (2010), pp. 91-108

[49] Rahman, A., Ullah, S.: Seismic vulnerability assessment of RC structures: A review, ATE-90214062, Asian Transactions, (2013) 1.

[50] Marasco, S., Noori, A.Z., Domaneschi, M., Cimellaro, G.P.: Seismic vulnerability assessment indices for buildings: Proposals, comparisons and methodologies at collapse limit states, Intern. J. of Disaster Risk Reduction, 63 (2021), pp. 1-15

[51] Alam, N. Shahria Alam, M., Tesfamariam, S.: Buildings' seismic vulnerability assessment methods: A comparative study, Nat Hazards, 65 (2012), pp. 405–424, https://doi.org/10.1007/s11069-011-0082-4

[52] Cherifi, F., Farsi, M., Kaci, S.: Assessment of seismic vulnerability of RC frame buildings, MATEC Web of Conferences 149, 2018.

[53] Lamantarna, E., Lam, N., Tsang, H.H., Wilson, J., Gad, E., Goldsworty, H.: Review of methodologies for seismic vulnerability assessment of buidings, Proceedings of the Australian Earthq. Engl. Society, Lorne, Victoria, 2014.

[54] Yaghmaeei-Sabegh, S., Zafavand, S., Makeremi, S.: Evaluation of N2 method for damage setimation of MDOF systems, Earthquake and Structures, 14 (2018) 2, pp. 155-165

[55] Xin, D., Daniell, J.E., Wenzel, F.: State of the art of fragility analysis for major building types in China with implementations for intensity – PGA relationship, Nat. Hazards Earth Syst. Sci. Discuss., 2018.

[56] Maeda, M., Nakano, Y., Lee, K.S.: Post-Earthquake damage evaluation for RC buildings based on residual seismic capacity, Proceedings of the13th WCEE, Vancouver, B.C., Canada, 2004.

[57] Martins, L., Silva, V., Merques, M., Crowley, H., Delgado, R.: Evaluation of analytical fragility and damage-to-loss models for reinforced concrete buildings, Proceedings of the Sec. Eur. Conf. on Earthquake Engl. and Seismology, 2014., pp. 12

[58] Hamburger, R.O., Hooper, J.D., Gillengerten, J. D., Dwelley-Samant, L., Heintz, J., Mahoney, M.: The ATC-58-2 Project Further Development of Next Generation Performance-based Design Criteria, Proceedings of the 16WCEE, Santiago de Chile, Chile, 2017.

[59] El-Betar, S.A.: Seismic vulnerability evaluation of existing RC buildings, HBRC J., 14 (2018), pp. 189-197

[60] Folić, R., Čokić, M.: Fragility and Vulnerability Analysis of an RC Building with the Application of Nonlinear Analysis, Buildings: Selected Papers from the 1st Croatian Conference on Earthquake Engineering (1CroCEE), 11 (2021) 9, pp. 390, https://doi.org/10.3390/buildings11090390

[61] Maio, R.A., Tsionis, G., Sousa, M.L., Dimova, S.L.: Review of fragility curves for seismic risk assessment of buildings in Europe, Proceedings of the 16th World Conference on Earthquake Engineering, Santiago Chile, Chile, 2017.

[62] Park, Y.J., Ang, A.H.S.: Mechanistic seismic damage model for reinforced concrete, J. Struct. Engl.,111 (1985), pp. 722–739

[63] Lađinović, Đ., Folić, R.: Application of imroved damage index for designing of earhquake resistant structures, Proceedings of the 13th World Conference on Earthquake Engineering, Vancccouver, B.C., Canada, 2004.

[64] Ambraseys, N., Smit, P., Sigbjornsson, R., Suhadolc, P., Margaris, B.: Internet-site for European Strong-motion Data, European Commission, Research-directorate General, Environment and Climate Programme, http://www.isesd.hi.is, 1.1.2021.

[65] ORFEUS: Engineering Strong Motion Database, https://esm-db.eu/, 11.1.2021.

[66] Fahjan, Y.M.: Selection and Scaling of Real Earthquake Accelerograms to Fit the Turkish Design Spectra, Digest, 19 (2008), pp. 1231–1250

[67] NIST GCR 11-917-15: Selecting and Scaling Earthquake Ground Motions for Performing Response-history Analyses, NEHRP Consultants Joint Venture for U.S. Department of Commerce National Institute of Standards and Technology Engineering Laboratory, Gaithersburg, MD, USA, 2011.

[68] Bisch, P., Carvalho, E., Degee, H., Fajfar, P., Fardis, M., Franchin, P., Kreslin, M., Pecker, A., Pinto, P., Plumier, A., et al.: Eurocode 8: Seismic Design of Buildings-Worked Examples, EC 8: Seismic Design of Buildings, Publications Office of the European Union, Lisbon, Portugal, 2012.

[69] Pazoki, M., Tasnimi, A.A.: Assessment of the Park & Ang Damage Index for Performance Levels of RC Moment Resisting Frames, Proceedings of the 7th International Conference on Seismology & Earthquake Engineering, 2015.

[70] Mohd, Z., Mohd, S., Sangle, K.K.: Seismic damage assessment of reinforced concrete structure using non-linear static analyses, KSCE Journal of Civil Engineering, 21 (2017) 4, pp. 1319-1330

[71] Pejović, J., Janković, S.: Seismic fragility assessment for reinforced concrete high-rise buildings in Southern Euro-Mediterranean zone, Bull. Earthq. Engl., 14 (2016), pp. 185–212

[72] Sinha, R., Shiradhonkar, S.R.: Seismic Damage Index for Classification of Structural Damage – Closing the Loop, Proceedings of the 15th World Conference on Earthquake Engineering, Lisbon, Portugal, 2012.

[73] Bastami, M., Ebrahimi, B.: Modification of Park-Ang Damage Index to Accommodate Effect of Aftershocks on RC Structures, Journal of Seismology & Earthquake Engineering, 21 (2019) 4, pp. 21-35

[74] Ghosh, S., Datta, D., Katakdhond, A.A.: Estimation of the Park–Ang damage index for planar multi-storey frames using equivalent single-degree systems, Engl. Struct., 33 (2011), pp. 2509–2524

[75] Ganjavi, B., Amiri, J.V., Amiri, G.G., Amrei, S.A.R.: Effect of Seismic Loading Patterns on Height-Wise Distribution of Drift, Hysteretic Energy and Damage in Reinforced Concrete Buildings, Journal of Applied Sciences, 22 (2007) 7, https://doi.org/10.3923/jas.2007.3431.3441

[76] Kassem, M.M., Nazri, F.M., Farsangi, E.N., Tan, C.G.: Comparative seismic RISK assessment of existing RC building, Structures, 32 (2021), pp. 889-913

[77] Vona, M.: Fragility curves of existing RC buildings based on specific structural performance levels, Open J. of Civil Engineering, (2014) 4, pp. 120-134

[78] Kassem, M.M., Nazri, F.M, Farsangi, E.N.: Development of seismic vulnerability index methodology for reinforced concrete buildings based on nonlinear parametric analysis, Methods, 10 (2019) 6, pp. 199-211

[79] Belheouane, F.I., Bensaibi, M.: Assessment of vulnerability curves using vulnerability index method for reinforced concrete structures, Intern. J. of Structural and Construction Engineering, 7 (2013) 6, pp. 483

[80] Kassem, M.M., Nazri, F.M., Farsangi, E.N.: The seismic vulnerability assessment methodologies: A State-of-the-Art Review, Ain Shams Engineering Journal, 11 (2020), pp. 849-864

[81] Kassem, M.M., Nazri, F.M., Farsangi, E.N., Oztuk, B.: Development of a uniform seismic vulnerability framework for reinforced concrete building typology, Journal of Building Engineering, 47 (2022), No. 103838

[82] Desai, K., Sheth, R., Patel, K.: Performance evaluation using fragility analysis of RC frame /wall structures, RT&A, 16 (2021) 1, pp. 187-195

[83] Computers and Structures Inc.: ETABS, version 17, https://www.csiamerica.com/, 11.1.2021.

[84] Applied Technology Council: ATC-40 Seismic Evaluation and Retrofit of Concrete Buildings, Report No. SSC 96-01, 1 (1996), https://www.atcouncil.org/pdfs/atc40toc.pdf, 11.1.2021.